

The adsorption of HCl on volcanic ash

Xochilt Gutiérrez, Federica Schiavi, Hans Keppler

▶ **To cite this version:**

Xochilt Gutiérrez, Federica Schiavi, Hans Keppler. The adsorption of HCl on volcanic ash. Earth and Planetary Science Letters, 2016, 438, pp.66-74. 10.1016/j.epsl.2016.01.019 . hal-02404351

HAL Id: hal-02404351
https://uca.hal.science/hal-02404351

Submitted on 11 Dec 2019

HAL is a multi-disciplinary open access archive for the deposit and dissemination of scientific research documents, whether they are published or not. The documents may come from teaching and research institutions in France or abroad, or from public or private research centers.

L'archive ouverte pluridisciplinaire **HAL**, est destinée au dépôt et à la diffusion de documents scientifiques de niveau recherche, publiés ou non, émanant des établissements d'enseignement et de recherche français ou étrangers, des laboratoires publics ou privés.

The adsorption of HCl on volcanic ash

Xochilt Gutierrez, Federica Schiavi, and Hans Keppler*

Bayerisches Geoinstitut, Universität Bayreuth, 95440 Bayreuth, Germany

*Corresponding author: hans.keppler@uni-bayreuth.de

Abstract. Understanding the interaction between volcanic gases and ash is important to derive gas compositions from ash leachates and to constrain the environmental impact of eruptions. Volcanic HCl could potentially damage the ozone layer, but it is unclear what fraction of HCl actually reaches the stratosphere. The adsorption of HCl on volcanic ash was therefore studied from -76 to + 150 ˚C to simulate the behavior of HCl in the dilute parts of a volcanic plume. Finely ground synthetic glasses of andesitic, dacitic, and rhyolitic composition as well as a natural obsidian from Vulcano (Italy) served as proxies for fresh natural ash. HCl adsorption is an irreversible process and appears to increase with the total alkali content of the glass. Adsorption kinetics follow a first order law with rate constants of $2.13 \cdot 10^{-6}$ s^{-1} to $1.80 \cdot 10^{-4}$ s^{-1} in the temperature range investigated. For dacitic composition, the temperature and pressure dependence of adsorption can be described by the equation $\ln c = 1.26 + 0.27 \ln p - 715.3/T$, where c is the surface concentration of adsorbed HCl in mg/m^2, T is temperature in Kelvin, and p is the partial pressure of HCl in mbar. A comparison of this model with a large data set for the composition of volcanic ash suggests that adsorption of HCl from the gas phase at relatively low temperatures can quantitatively account for the majority of the observed Cl concentrations. The model implies that adsorption of HCl on ash increases with temperature, probably because of

the increasing number of accessible adsorption sites. This temperature dependence is opposite to that observed for SO_2, so that HCl and SO_2 are fractionated by the adsorption process and the fractionation factor changes by four orders of magnitude over a temperature range of 250 K. The assumption of equal adsorption of different species is therefore not appropriate for deriving volcanic gas compositions from analyses of adsorbates on ash. However, with the experimental data provided here, the gas compositions in equilibrium with the ash surfaces can be calculated. In particular, for dacitic composition, the molar ratio of S/Cl adsorbed to the ash surface is related to the molar S/Cl ratio in the gas phase according to the equation $\ln (S/Cl)_{adsorbed} = 2855\ T^{-1} + 0.28 \ln (S/Cl)_{gas} - 11.14$. Our data also show that adsorption on ash will significantly reduce the fraction of HCl reaching the stratosphere, only if the initial HCl content in the volcanic gas is low (< 1 mole %). For higher initial HCl concentrations, adsorption on ash has only a minor effect. While HCl scavenging by hydrometeors may remove a considerable fraction of HCl from the eruption column, recent models suggest that this process is much less efficient than previously thought. Our experimental data therefore support the idea that the HCl loading from major explosive eruptions may indeed cause severe depletions of stratospheric ozone.

Keywords: Adsorption, ash, hydrogen chloride, volcanic gases, ozone

1. Introduction

The short-term climatic impact of volcanic eruptions is mostly due to the interaction of sulfur and halogen species in volcanic gases with the atmosphere. The surface cooling observed after major explosive eruptions is caused by the injection of sulfur dioxide into the stratosphere, where it is photochemically oxidized to sulfate aerosols.

These aerosols backscatter sunlight and may remain in the stratosphere for months or even years (e.g. McCormick et al. 1995, Robock 2000). Ozone destruction is another potential effect of large explosive eruptions, but it is much less understood than the surface cooling effect. Black et al. (2014) suggested that the end-Permian mass extinction partially resulted from ozone depletion associated with the Sibirian Trap magmatism. Measurable depletions in stratospheric ozone were observed after the 1991 Mt. Pinatubo eruption (Brasseur and Granier 1992, Solomon et al. 1998). They were attributed to the catalytic effect of sulfate aerosol surfaces, which may enhance the concentration of active chlorine species involved in ozone destruction (Solomon et al. 1993, Hofmann et al. 1994). However, another mechanism could be the direct injection of volcanic hydrogen chloride (HCl) into the stratosphere. A study by Tabazadeh and Turco (1993) suggested that this mechanism is inefficient, because hydrogen chloride would be nearly completely washed out of the eruption column by condensing water. More recent models of eruption plumes (Textor et al. 2003), however, show that most of the water in the plume is present as solid ice, which greatly reduces the efficiency of HCl scavenging. Moreover, most of the ice particles are lifted upwards, so that more than 25 % of the HCl originally contained in the plume may reach the stratosphere. This prediction was confirmed for the case of a high-latitude eruption by direct sampling of a volcanic cloud from Hekla volcano (Rose et al. 2006, Millard et al. 2006). Spectroscopic observations also suggested an increase of 40 % in the total column of HCl above 12 km altitude after the 1982 El Chicón eruption (Mankin and Coffey 1984, see also Woods et al. 1985), while at most a slight increase in stratospheric HCl was observed after the 1991 Mt. Pinatubo eruption (Mankin et al. 1992, Wallace and Livingston 1992). Kutterolf et al. (2013) estimated the Cl and Br release from 14 large explosive eruptions in Nicaragua in the

last 70 00 years and concluded that most of these eruptions likely caused significant ozone destruction in the stratosphere. On the other hand, elevated HCl concentrations are only rarely detected in ice cores; this may, however, be due to the volatilization of HCl in the presence of H_2SO_4 (Wagnon et al., 1999, Zdanowicz et al. 1999, Thamban et al. 2006). The limited data available may imply that the stratospheric HCl yield of eruptions varies considerably, depending on initial gas composition and on the processes occurring in the eruption column.

Hydrogen chloride (HCl) concentrations in volcanic gases typically range from < 0.05 to > 5 mole %, with most data probably in the 0.1 to 1 mole % range (Symonds et al. 1994, Fischer 2008). Relatively high HCl concentrations and HCl/SO_2 ratios are often found in arc volcanoes. Estimated annual fluxes of HCl vary widely, from 0.4 to 170 Tg/a (Symonds et al. 1988, Halmer et al. 2002). Pyle and Mather (2009) used a compilation of measured HCl/SO_2 ratios and total SO_2 fluxes to estimate the HCl flux from arc volcanoes at 4.3 ± 1 Tg/a, which is believed to dominate the global flux. However, the flux of HCl reaching the stratosphere is certainly much lower, because only large eruptions penetrate the tropopause and processes in the eruption column may deplete HCl. While the depletion by water and ice has already been investigated in some detail, little is known about the possible effect of HCl adsorption on volcanic ash (Rose 1977). Ayris et al. (2014) studied the interaction of HCl with ash under near-vent, high-temperature conditions (200 - 800 ˚C). Only for alkali-rich tephrite and phonolite glasses, reaction with HCl to NaCl was observed, but not for dacite and rhyolite. The very short residence time of ash at near-vent conditions during an explosive eruption may further limit the extent of adsorption at high temperature. This suggests that HCl adsorption, if it is an important process at all, must occur in the

101 low-temperature portion of the dilute plume. We therefore studied the adsorption of
102 HCl on ashes of rhyolitic, dacitic, and andesitic composition from -76 to + 150 ˚C at
103 variable HCl partial pressures covering the plausible conditions in a dilute volcanic
104 plume.
105
106 **2. Experimental methods**
107 Fe-free synthetic glasses of rhyolitic, dacitic, and andesitic composition were used as
108 proxies for fresh volcanic ash. The glasses were prepared from homogenized,
109 stoichiometric mixtures of analytical grade SiO_2, $Al(OH)_3$, MgO, $CaCO_3$, Na_2CO_3,
110 and K_2CO_3. After decarbonation in a platinum crucible, the charge was melted at
111 1600 ˚C for 1 hour and quenched in deionized water, yielding a clear glass with some
112 bubbles. Microprobe analyses are given in Table 1. The glass was then dried and
113 ground four times for seven minutes each in a planetary mill. No liquid was added to
114 avoid adsorption on fresh surfaces. The surface area of the powders was determined
115 with a Quantachrome instrument by measuring the BET adsorption isotherm of
116 krypton at 77 K. To constrain the isotherm, seven data points were measured in a
117 range of pressures ranging from 5 to 30 % of the condensation pressure of Kr. 100 –
118 200 mg of sample were outgassed at 200 ˚C for 24 hours before the measurement.
119 The specific surfaces obtained were in the range of 1.5 – 4.9 m^2/g. These numbers are
120 quite comparable to those obtained for fine (< 100 μm) natural ash (mostly 1.1 – 2.1
121 m^2/g for a sieved fraction < 100 μm; Demelle et al. 2005; 4.3 m^2/g for
122 phreatomagmatic ash from Eyafjallajökull; Gislason et al. 2011).
123
124 Adsorption measurements were carried out in a glass apparatus equipped with a
125 Vacuubrand DVR 5 pressure gauge, following the procedure described by Schmauss

and Keppler (2014). In brief, 30 – 50 g of the sample powder were placed in a sample tube and the entire system was evacuated. HCl gas was then filled into a reservoir flask up to the desired pressure. Once the valve between the sample tube and the reservoir was opened, an instantaneous pressure drop occurred due to the expansion of the gas into the sample tube, followed by a slow decrease in pressure due to the adsorption of HCl on the sample surface. From the known volumes of the system, the measured pressure drop and the temperature, the amount of adsorbed HCl can be calculated. All required formulae are given by Schmauss and Keppler (2014). For calculating the amount of adsorbed HCl, the ideal gas law was used, which is a very good approximation for HCl under the low pressures and the temperatures of interest. Once the pressure in the system had stabilized, the valve between sample and gas reservoir was closed and the pressure in the reservoir was increased. After opening the valve again, the next point of the adsorption isotherm was measured. This procedure was repeated until the pressure in the system reached nearly one bar. Desorption experiments started from close to one bar by decreasing the pressure in the reservoir with a vacuum pump. After opening the valve to the sample, pressure first increased, due to expansion of the gas from the sample tube to the reservoir, followed by a slow increase due to desorption of HCl from the sample surface. After pressure stabilized, the valve between reservoir and sample was closed and the procedure was repeated, until the pressure in the reservoir was close to zero mbar. Measuring an entire adsorption and desorption cycle for a sample took several weeks. Experiments at 150 ˚C were carried out by immersing the sample tube in an oil bath; for experiments at – 76 ˚C, the sample tube was cooled with a mixture of dry ice and acetone. Main sources of error in the surface concentrations are the specific surfaces of the powders, the pressures, and the volumes in the system.

Wet chemical analyses were carried out in order to confirm the measured HCl surface concentrations. About 10 g of HCl-loaded glass sample were mixed with 100 ml of distilled water and stirred for 24 hours in a closed Erlenmeyer flask. The solution was then filtered off and some $NaHCO_3$ added to adjust to neutral pH. Chloride was then determined by titrating against a 0.1 N $AgNO_3$ solution with Ag_2CrO_4 as endpoint indicator (Mohr method). Surface concentrations (in mg/m^2) were then obtained by dividing the mass of measured HCl by the surface area of the sample according to the BET data.

3. Results

3.1. Kinetics of adsorption

Figure 1 shows the experimentally observed decrease of pressure during an adsorption experiment. For every adsorption step, the data can be described by an equation

$$(p - p_{eq}) = (p_0 - p_{eq})\, e^{-\lambda t} \qquad (1)$$

where p is pressure, p_{eq} is the equilibrium pressure, and p_0 is the initial pressure after opening the valve between gas reservoir and sample; λ is the rate constant and t is time. Values of p_{eq} and of λ were obtained by fitting equation (1) to the data for every adsorption step. Since in the ideal gas law, pressure is proportional to the number of moles in the gas phase, $(p - p_{eq})$ is proportional to the number of gas atoms n that still will be absorbed and $(p_0 - p_{eq})$ is proportional to the initial number of gas atoms n_0

that ultimately will end up on the sample surface. The above equation (1) is therefore equivalent to a first-order-law of reaction kinetics

$$n = n_0 e^{-\lambda t} \qquad (2)$$

with the same rate constant λ as in equation (1).

Experimentally determined rate constants are compiled in Table 2; measured values for λ range from $2.13 \cdot 10^{-6}$ s^{-1} to $1.80 \cdot 10^{-4}$ s^{-1}. The timescale for reaching equilibrium is in the order of magnitude of the inverse of these rate constants. For dacite at room temperature, a clear decrease of λ with the initial gas pressure of the adsorption experiment is observed. This may be related to the fact that in the experiments at higher pressure, the most reactive surface sites had already been saturated with HCl in the previous steps of the adsorption experiment. In other words, with increasing surface coverage of the sample, the rate of adsorption decreases. This effect is not so clearly seen for the other samples. Interestingly, the rate constants for HCl adsorption on dacite at -76 ˚C are in most cases higher than at room temperature. This is unexpected, as reaction rates should generally increase with temperature. However, as will be discussed below, only the most reactive surface sites seem to be accessible for HCl adsorption at – 76 ˚C, and this higher reactivity probably also translates into higher rate constants. Desorption experiments also followed a first-order-kinetics, with rate constants similar to those for adsorption on the same sample. However, only very little desorption was generally observed and therefore, desorption kinetics will not be further discussed.

3.2. Adsorption isotherms

Adsorption and desorption isotherms of HCl for andesitic, dacitic and rhyolitic glasses are shown in Figure 2. With increasing pressure, the amount of HCl adsorbed on the surface first increases sharply and then levels off and reaches a plateau. This behavior corresponds to a type I adsorption isotherm in the Brunauer classification (Brunauer et al. 1940), which is typical for a chemisorption process, where the adsorbed molecule forms strong chemical bonds with the substrate. Above about 500 mbar, there is a slight further increase in surface concentration that may indicate minor multilayer adsorption.

The desorption isotherms show that the adsorption process is nearly irreversible, i. e. the surface concentration of HCl remains nearly constant when pressure is decreased to zero mbar. This behavior is again consistent with a chemisorption process involving the formation of strong chemical bonds between HCl and the substrate. The HCl surface concentration observed for andesitic and rhyolitic glasses are rather similar, while those for the dacite glass are 2 to 3 times higher. Inspection of Table 1 shows that this effect cannot be due to the SiO_2, Al_2O_3, CaO or MgO contents of the glass, since the percentage of these components in the dacite glass is between that for rhyolite and andesite. However, the total alkali ($Na_2O + K_2O$) content of the dacite is significantly higher than for the other two compositions. Since the alkalis are the strongest bases in the system, it is plausible that they enhance the reaction with the acidic HCl molecule. This is consistent with the enhanced reactivity of alkali-rich glasses with HCl vapor at high-temperature, near vent conditions (Ayris et al. 2014). Note, however, that the alkali contents of the synthetic glasses used for this study are

224 not necessarily representative of a global average of rhyolite or dacite compositions
225 and individual rhyolites may very well have higher total alkalis than some dacites.
226
227 The temperature dependence of HCl adsorption was explored for dacite, by carrying
228 out additional experiments at -76 ˚C and at 150 ˚C. The results are shown in Figure 3.
229 Adsorption increases with temperature, probably because at low temperature
230 adsorption occurs only on some particularly reactive sites, with the number of
231 available sites increasing with temperature. This is a typical behavior sometimes
232 observed for chemisorption, where the formation of chemical bonds requires some
233 activation energy that can only be overcome above a certain temperature (e.g. Batzill
234 2006, Duran-Munoz et al. 2013).
235
236 The surface concentrations of HCl remaining on the samples after the end of the
237 desorption experiments, as derived from the measurements of the isotherms, were
238 checked by argentometric titration of leachate solutions, with generally good
239 agreement (Supplementary Table S1). Only the dacite sample from the experiment at
240 room temperature may have lost some HCl by handling on humid air before the
241 argentometric analysis. For the comparison, the surface concentrations were
242 converted into wt. % using the specific surfaces given in Table 1.
243
244 *3.3. A regression model for the adsorption of HCl on dacite glass*
245 Schmauss and Keppler (2014) showed that the temperature and pressure dependence
246 of the adsorption of SO_2 on volcanic ash may be described by a modified Freundlich
247 isotherm
248

$$\ln c = A\,T^{-1} + B \ln p + C \qquad (3)$$

where c is the surface concentration in mg/m^2, T is temperature in K and p is the partial pressure of the absorbed gas in mbar. A least squares fit of all the experimental data for HCl adsorption on dacite glass using the same equation yielded A = -715.3 ± 55.3, B = 0.27 ± 0.03, and C = 1.26 ± 0.29, with R^2 = 0.93. A comparison of measured and predicted surface concentrations of HCl is shown in Figure 4.

3.4. HCl adsorption on a natural obsidian sample

In order to test whether the adsorption data obtained by using synthetic samples are also applicable to natural, Fe-bearing volcanic glasses, we also measured the adsorption of HCl on a natural alkali-rhyolitic obsidian from the 1739 AD eruption of Vulcano (Aeolian Islands, Italy; see Table1). This obsidian contains a small fraction of feldspar microlites. In adsorption experiments at room temperature, both the kinetics of adsorption and the adsorption isotherm were found to be quite similar to the synthetic glasses (Fig. 5). The HCl surface concentrations observed for the Vulcano obsidian are somewhat higher than for the synthetic rhyolite and resemble more those for synthetic dacite (Fig. 2). This is, however, entirely consistent with the elevated bulk alkali content in this sample, supporting the idea that this is the primary compositional parameter influencing HCl adsorption.

4. Discussion

4.1. Applicability of the experimental data to adsorption in volcanic plumes

The experiments in the present study were carried out in the presence of HCl alone, while in the volcanic plume, H_2O is usually the most abundant component, together with smaller amounts of SO_2, HCl and traces of other gases. CO_2 may be an abundant species as well, but since the CO_2 molecule lacks a permanent dipole moment, its absorption on surfaces can likely be ignored. The much more important question is therefore, whether the data obtained in the present study may be applied to the situation in a volcanic plume, where HCl is a minor component compared to H_2O. Very likely this is possible, because the glass powders used in the experiments described here were exposed to air of average humidity at ambient conditions during the preparation of the experiments. Both studies on synthetic silicate glasses and of volcanic ashes show that under ambient conditions and also in a volcanic plume, the surface of a glass particle will be covered with a complete layer of adsorbed H_2O molecules (Razouk and Salem 1948, Delmelle et al. 2005). Accordingly, there should be no difference in HCl surface concentration between the glass powders studied here in pure HCl alone and the adsorption of HCl on ash in the volcanic plume. Dissolution of HCl gas in liquid water adhering to ash particles is a separate effect, which will be discussed below.

Figure 6 compares Cl concentrations adsorbed on the surface of volcanic ashes from more than 40 individual eruptions with the experimental data for dacite glass obtained in this study. To convert surface concentrations (in mg/m^2) into bulk concentrations (mg Cl / kg ash), the specific surface area of the ash has to be assumed. Figure 6 shows predicted maximum bulk concentrations (vertical lines) for two different specific surfaces of 1 m^2/g, which is at the low end of this parameter for fine ash (Demelle et al. 2005; Gislason et al. 2011) and 0.1 m^2/g, more characteristic for

coarser ash (see supplementary Table S2 for examples). The vertical lines in Figure 6 give maximum concentrations achievable at a given specific surface and temperature at high HCl partial pressures. However, inspection of Figure 3 shows that similar concentrations may already be reached at low HCl partial pressures (10 - 100 mbar) realistic for a volcanic plume. Figure 6 shows that adsorption of HCl from the gas phase can account for the vast majority of the observed Cl concentrations. Only the data for Irazu and San Miguel appear anomalously high, but they could still be explained by surface adsorption if the specific surface of these ashes were higher, in the order of 2 – 4 m^2/g, within the range confirmed by measurements on fine ashes (Demelle et al. 2005; Gislason et al. 2011). More likely, however, theses ashes contain Cl from some other source, e.g. from hydrothermal alteration. Alteration processes may also have contributed some Cl to other samples. The data shown in Figure 6 are completely consistent with earlier experimental results for fluorine. Oskarsson (1980) already concluded that the fluorine concentrations adsorbed on ash may be explained by adsorption from the gas phase at relatively low temperatures near 200 ˚C.

In a volcanic plume, ash may interact with aerosols or become coated by films of liquid water or ice. Rose (1977) suggested that the accumulation of aerosol particles, particularly of H_2SO_4 is a main source for adsorbed material on ash. However, H_2SO_4 aerosols are usually only a minor species, subordinate to SO_2 in volcanic plumes close to the vent (e.g. Mather et al. 2006). Delmelle et al. (2007; see also Gislason et al. 2011) detected Cl and S on the surface of ash particles by X-ray photoelectron spectroscopy, but not by SEM. They concluded that Cl and S form coatings with a thickness of a few nm at most; they further suggested that this observation together

with the observed surface depletion in Na, K, Mg, and Ca argues against the deposition of material via aerosols, but is more consistent with precipitation from a liquid film. However, their data are equally consistent with our model of direct adsorption from a gas phase, since the shape of the adsorption isotherms indeed suggests the formation of a mono-molecular layer of HCl on the ash surface. Coating of ash particles by water certainly occurs in some parts of the plume, but this process is reversible. Once the water evaporates, the dissolved HCl and SO_2 will also be lost, unless some surface reaction has occurred. However, if the surface is in equilibrium with the liquid film and the liquid is in equilibrium with a gas phase, then the surface is also in direct equilibrium with the gas. In other words, this process should lead to the same surface concentration as observed in our experiments. The fact that surface reactions, but not the solubility in liquid water determine the origin of leachable material on ash surfaces is also supported by the observation of a systematic offset between S/Cl ratios adsorbed on ash and S/Cl ratios in rainwater (Edmonds et al., 2003). If the relative solubility of SO_2 and HCl in liquid water somehow determined the S/Cl ratio on the ash surface, this ratio should be the same as in rainwater that had interacted with the plume.

4.2 Deriving volcanic gas compositions from adsorbate analyses

The analysis of volatile species adsorbed on fresh ash surfaces is a convenient and frequently used method to infer volcanic gas compositions (e.g. Rose 1977, Williams et al. 1986, Armienta et al. 1998, de Hoog et al. 2001, Armienta et al. 2010, Bagnato et al. 2011, 2013). Usually, the implicit assumption is made that the concentration ratio of adsorbed S, Cl, and F is somehow comparable to the molar ratio of the

corresponding species in the gas phase of the plume. Our experimental data, together with published results for the adsorption of SO_2 on volcanic ash (Schmauss and Keppler, 2014) allow testing this assumption. The adsorption of HCl and SO_2 can likely be treated independently, without considering direct interactions, because the concentration of these gases, particularly in the dilute part of the plume, is very low and therefore, none of them will fully cover the glass surface. Moreover, the experimental data of this study and of Schmauss and Keppler (2014) suggest that HCl and SO_2 actually react with different surface sites, since both the dependence of adsorption on glass composition and on temperature are very different. For SO_2, glass composition has little influence on adsorption, while the total alkali content seems to control the reactivity with HCl. HCl adsorption increases with temperature, while the adsorption of SO_2 decreases with temperature.

Schmauss and Keppler (2014) showed that SO_2 adsorption on dacite glass can be described by the equation

$$\ln c_{SO2} = 2140\ T^{-1} + 0.29 \ln p_{SO2} - 9.32 \qquad (4)$$

while in the present study, we observed that HCl adsorption follows the equation

$$\ln c_{HCl} = -\ 715.3\ T^{-1} + 0.27 \ln p_{HCl} + 1.26 \qquad (5)$$

In both equations, the coefficient in front of the ln p term is indistinguishable within experimental error. If one assumes an average coefficient of 0.28, both equations can be combined to

374

375 $$\ln (c_{SO2}/c_{HCl})_{adsorbed} = 2855\ T^{-1} + 0.28 \ln (p_{SO2}/p_{HCl}) - 10.58 \qquad (6)$$

376

377 At the low pressures involved, the ratio of the partial pressures p_{SO2}/p_{HCl} is virtually
378 identical with the SO_2/HCl molar ratio in the gas. To convert the ratio of surface
379 concentrations c_{SO2}/c_{HCl}, which are given in mg/m^2, into a molar ratio of S/Cl, the
380 numbers have to be divided by the ratio of the molar masses of SO_2 and HCl. This
381 adds a linear term of - ln (64.06/36.46) = - 0.56 to the equation, which then becomes:

382

383 $$\ln (S/Cl)_{adsorbed} = 2855\ T^{-1} + 0.28 \ln (S/Cl)_{gas} - 11.14 \qquad (7)$$

384

385 where S/Cl now refers to the molar ratio in the gas and on the glass surface.

386

387 Figure 7 shows the ratio of S/Cl on dacitic ash surfaces, as predicted by equation 7 for
388 a range of temperatures and gas compositions. Obviously, the adsorbed S/Cl ratio is a
389 very strong function of temperature. In fact, the temperature effect is much stronger
390 than the effect of the S/Cl ratio in the gas. For example, near 0 ˚C, increasing the S/Cl
391 ratio in the gas by a factor of 10 has the same effect on the absorption as reducing
392 temperature by less than 20 ˚C. The relatively small effect of gas composition is due
393 to the factor of 0.28 in front of the $\ln (S/Cl)_{gas}$ term in equation (7); it implies that
394 under otherwise equal conditions, (S/Cl) in the adsorbate only increases by a factor of
395 $(S/Cl)_{gas}^{0.28}$, i.e. a 10-fold increase in this ratio in the gas phase only translates into a
396 less than 2-fold increase in the adsorbate. The 0.28 exponent is related to the effect
397 seen in Figure 2 that the amount of adsorbed HCl first increases sharply at low p_{HCl},
398 but then levels off at higher p_{HCl}. The strong effect of temperature on the adsorbed

399 S/Cl ratio is obviously related to the opposite temperature dependence for HCl and
400 SO_2 adsorption. The decrease of adsorption with temperature for SO_2 (Schmauss and
401 Keppler 2014) is the normal behavior expected for adsorption. This is because in the
402 expression for the Gibbs free energy $\Delta G = \Delta H - T\Delta S$ for the adsorption reaction, the
403 $-T\Delta S$ term increases with temperature and should therefore shift the equilibrium to
404 the side with higher entropy; the entropy of a molecular species is always higher in
405 the gas phase than adsorbed on a surface. The increase in HCl adsorption with
406 temperature is therefore very unusual, but this kind of behavior is sometimes observed
407 for chemisorption (e.g. Batzill 2006, Duran-Munoz et al. 2013), i.e. if the adsorption
408 process involves the formation of strong chemical bonds. In such a situation, an
409 activation energy may have to be overcome for the reaction, so that only a fraction of
410 sites is involved in the adsorption process at low temperature, while this fraction
411 increases at higher temperatures. Once all possible surface sites are activated,
412 adsorption should decrease upon further increase with temperature, because of the
413 thermodynamic argument mentioned above. Accordingly, the data presented here for
414 HCl adsorption and equation 7 should not be extrapolated to temperatures far above
415 those for which they were calibrated (i.e. beyond 150 ˚C).
416
417 The strong temperature effect on adsorption as shown in Figure 7 needs to be taken
418 into account whenever volcanic gas compositions are to be derived from analyses of
419 volatile species adsorbed on ash surfaces. This means that estimates of volcanic fluxes
420 of HCl that were obtained from SO_2 flux measurements scaled by the S/Cl ratio in
421 adsorbates should be treated with considerable caution; the same may also apply to
422 other gas species. The frequently made assumption of equal adsorption of different
423 species is only valid under very specific conditions (see also Bagnato et al. 2011). For

example, Figure 7 shows that for a gas with an S/Cl ratio of 1, equal adsorption, resulting in an S/Cl ratio of 1 also in the adsorbate, only occurs at a temperature near – 20 ˚C. However, for an S/Cl ratio in the gas of 10, the temperature where no fractionation occurs decreases to near – 50 ˚C.

The conclusions reached here on the strong effect of temperature on the fractionation of SO_2 and HCl during adsorption are actually quite consistent with a number of field observations. S/Cl ratios of ashes vary widely, < 0.01 to > 100, and often by orders of magnitude even within the same eruption (see Supplementary Table 2). This is likely not only due to variations in gas composition, but also to the fractionation of S and Cl between gas and ash. Edmonds et al. (2003) measured the SO_2/HCl ratio of gases from three eruption periods of the Soufrière Hills volcano on Montserrat between 1996 and 2002, using both open path infrared spectroscopy and the analysis of ash leachates. For the phase I and phase II major dome building periods, a SO_2/HCl molar ratio near 0.1 was spectroscopically detected in the plume and ash analyses gave similar (although more scattered) numbers. This is consistent with Figure 7, which suggests that for an S/Cl ratio of 0.1, no fractionation occurs between ash and gas phase near + 30 ˚C – a very plausible temperature for a low-altitude tropospheric plume in a tropical climate. Bagnato et al. (2013) studied ash leachates of the 2010 Eyafjallajökull eruption on Iceland and found major discrepancies between the S/Cl ratio adsorbed on ash surfaces and that measured in the volcanic gases. For the highly explosive phase III eruption, S/Cl ratios from ash leachates are mostly between 0.4 and 0.6, while direct gas measurements yielded significantly higher molar S/Cl ratios of 1.5 – 3.3. Inspection of Figure 7 suggests that these data may be reconciled by assuming a temperature of adsorption near 0 ˚C, quite plausible for a tropospheric

449 plume during spring in Iceland. Note that these ash samples were taken at horizontal
450 distances from the vent up to more than 50 km, where the plume will have cooled
451 down to ambient atmospheric temperature; closer to the vent, larger variations in
452 adsorbed S/Cl ratio are observed, which may be related to variations in plume
453 temperature and also plume height (4 – 9 km; Petersen et al. 2012). Even larger
454 fractionations of S and Cl between ash and gas were observed for the basaltic fire
455 fountain phase; the S/Cl ratio in the gas was measured to be between 5 and 25 while a
456 molar ratio of S/Cl of 0.14 was measured on the ash. According to Figure 7, this could
457 imply equilibration between gas and ash at temperatures around + 50 ˚C, which is
458 plausible for a fire fountain eruption, as there may be very significant radiative
459 heating of particles after they left the vent and the plume likely entrained less ambient
460 air than for the highly explosive phase III.
461
462 In the previous discussion, we have referred to Figure 7, which is based on equation 7
463 and strictly valid only for a dacitic composition. Glass composition will have some
464 effect on the S/Cl fractionation, which needs to be considered. However, this effect is
465 much smaller than the variation due to temperature. For a given gas composition,
466 Figure 7 suggests variations in the ratio of adsorbed S and Cl by four orders of
467 magnitude over just 250 ˚C. Compared to this, the compositional effect on the amount
468 of adsorbed HCl (Fig. 2) is only about a factor of 2 and the effect of glass
469 composition on SO_2 adsorption is even smaller (Schmauss and Kepper 2014).
470 Therefore, we believe that the conclusions derived from comparing the curves in
471 Figure 7 with ash leachate analyses are at least approximately correct, although
472 additional calibrations of the effect of ash composition on the S/Cl fractionation
473 between plume gas and ash surface are certainly desirable. In general, our discussion

474 shows that a large part of the apparent discrepancies between gas composition and the
475 composition of gas leachates can be accounted for by the effect of temperature on
476 adsorption. This does not rule out that other factors, in particular alteration processes
477 may also be important under some circumstances. However, for fresh, unaltered ash it
478 may indeed be possible to derive gas compositions from leachate analyses, if
479 reasonable estimates of plume temperature can be made. Moreover, on a local scale
480 close to a vent, the S/Cl ratio may actually provide a sensitive thermometer for the
481 temperature in the plume.
482
483 *4.3. Stratospheric HCl yield and ozone depletion*
484 With the experimental data on HCl adsorption obtained in this study, the fraction of
485 volcanic HCl reaching the stratosphere during Plinian eruptions can be better
486 constrained. As noted above, HCl adsorption increases with temperature, at least up to
487 150 ˚C. Accordingly, one may suspect that most of the adsorption may occur in the
488 relatively hot parts of the volcanic plume. However, ascent velocities in a typical
489 Plinian eruption column are > 100 m s^{-1} (Textor et al. 2006), implying that ash
490 particles reach the stratosphere within 1 – 2 minutes. This very much limits the time
491 available for high-temperature, near-vent interaction between volcanic gases and ash.
492 The highest rate constant for HCl adsorption measured in this study (Table 4) was 1.8
493 $\cdot 10^{-4}$ s^{-1}. For a residence time of 120 s, this would allow only 2 % of the equilibrium
494 surface concentration to be adsorbed on the ash. Accordingly, it is likely that most of
495 the adsorption occurs in the dilute parts of the volcanic plumes after it has cooled
496 down to the ambient temperature at the respective altitude.
497

A rough estimate of the magnitude of HCl adsorption can be obtained by considering the HCl surface concentration that would result from the (hypothetical) total adsorption of all the HCl in the plume. This concentration is simply the ratio of the total mass of HCl in the plume to the total available surface area of the ash. According to Woods and Bursik (1991) fine ash with a grain size < 100 μm accounts for > 50 wt. % of total deposit for Plinian eruptions. Measurements of fine ash samples from various volcanoes yielded specific surfaces of 1.1 – 2.1 m^2 / g (Delmelle et al. 2005). The ash is produced by the exsolution of gas bubbles, which ultimately disrupt and fragment the melt. Subduction zone magmas that are responsible for the most prominent explosive eruptions typically have pre-eruptive water contents near 5 wt. % (e.g. Métrich and Wallace 2008). Water is also the main component of the gas plume, with HCl concentrations ranging from < 0.05 to > 5 mole %, the majority of data probably being in the 0.1 to 1 mole % range (Symonds et al. 1994, Fischer 2008). These data from volcanic gases are in rough agreement with the Cl/ H_2O ratio in melt inclusions from primitive arc basalts (Métrich and Wallace 2008). If one therefore assumed a mass ratio of volcanic gas to (glassy) ash of 0.05 (equivalent to 5 % H_2O in the pre-eruptive magma), 1 mole % HCl in the gas and a surface of 1 m^2/g for the total ash (or 50 % of fine ash with 2 m^2/g), adsorbing all the HCl on the ash would yield a surface concentration of 1.01 mg/m^2. Comparing this number to the experimental data in Figure 2 and 3 suggests that such surface concentrations may be easily reached at room temperature or above; however, they may not be achievable at the much lower temperatures prevailing in the stratosphere. The situation would be very different, however, for an initial HCl concentration in the gas of 0.1 mole %; the corresponding surface concentration of 0.10 mg/m^2 is easily reached even at low temperatures and at low HCl partial pressure. This rough calculation already shows

523 that the initial HCl concentration in the plume, which likely reflects the pre-eruptive
524 Cl/H_2O ratio in the magma, largely controls the fraction of HCl sequestered by ash
525 and therefore, together with scavenging by hydrometeors, the effective stratospheric
526 HCl loading.
527
528 For a fully quantitative treatment of HCl adsorption, the equilibrium between the gas
529 phase and ash surface as described by equation (5) has to be considered together with
530 mass balance constraints under the conditions prevailing in the umbrella part of a
531 volcanic plume. For our calculations, we assume a plume model similar to that
532 described by Textor et al. (2006). The umbrella part of the plume is located at an
533 altitude near 20 km with a temperature around 220 K, containing about 100 g of ash
534 per kg of plume mixture. Assuming an initial gas mass fraction in the erupting
535 material of 5 wt. % (see above), this implies a dilution of volcanic gases by entrained
536 air by a factor of 200. The calculations are, however, rather insensitive to this dilution
537 factor, since according to equation (5), adsorption only increases with $p_{HCl}^{0.27}$, i.e. a
538 ten-fold increase in the dilution factor would only decrease adsorption by a factor of
539 1.9. For a volcanic gas with 1 mole % HCl, the partial pressure of HCl decreases from
540 10 mbar at the vent to 0.0022 mbar in the umbrella cloud by the combined effects of
541 the increasing altitude and dilution by entrained air. This number does not include
542 possible scavenging of HCl by hydrometeors (see Textor et al. 2003). Under the given
543 conditions, equation (5) predicts a concentration of HCl adsorbed on the surface of
544 ash of 0.026 mg/m^2 in equilibrium with this HCl partial pressure, less than 3 % of the
545 1.01 mg/m^2 required for total adsorption (see above). Since during the adsorption
546 process, the partial pressure of HCl in the gas decreases until equilibrium is reached,
547 the real number for the equilibrium surface concentration is slightly smaller.

548 Following the method described by Schmauss and Keppler (2014), one obtains
549 virtually the same value of 0.026 mg/m^2. This number appears small, but the resulting
550 bulk Cl concentration (26-52 mg/kg for a specific surface of 1-2 m^2/g) overlaps well
551 with the low end of concentrations reported for natural ashes (Fig. 6). Stratospheric
552 ash samples are likely under-represented in Figure 6, because many eruptions did not
553 reach the stratosphere and even for large eruptions, the ashes likely contain particles
554 that did not reach the stratosphere. For less explosive eruptions, particle velocities are
555 smaller and the plume may be less diluted by entrained air. Ash might therefore be
556 exposed to higher HCl partial pressures for longer times and at higher temperatures,
557 leading to stronger adsorption. This is a possible explanation for the fact that the
558 surface concentrations predicted for adsorption in the stratosphere are at the lower end
559 of the data for natural ash samples. However, the physical conditions for adsorption
560 likely vary considerably between individual eruptions and are influenced by
561 parameters such as the actual wind field that are hard to include in general models.
562
563 The calculation above clearly shows that for high initial HCl concentrations (> 1
564 mole %) in the gas phase of a Plinian eruption, adsorption by ash does not
565 significantly reduce the stratospheric HCl loading. However, the adsorption effect
566 becomes significant for low initial HCl concentrations. For example, for an initial
567 HCl content in the volcanic gas of 0.1 mole %, an equilibrium surface concentration
568 of 0.013 mg/m^2 is obtained, 13 % of the value required for total absorption (see
569 above). The relationship between HCl content in the initial volcanic gas and the
570 adsorption on ash is illustrated in Figure 8. Physically, this relationship is due to the
571 fact that the total amount of HCl in the plume increases proportionally to the initial
572 HCl molar fraction and therefore the HCl partial pressure; however, the amount of

573 HCl adsorbed on ash only increases with $p_{HCl}^{0.27}$ so that at higher p_{HCl}, the fraction of
574 HCl that is not removed by adsorption increases. In general, the efficiency of
575 adsorption on ash surfaces in dilute eruption plumes is much smaller for HCl than for
576 SO_2 (Schmauss and Keppler 2014).
577
578 The pre-eruptive Cl contents and Cl/H_2O ratios in subduction zone volcanics tend to
579 be high (Métrich and Wallace 2008, Kutterolf et al. 2013). Accordingly, HCl contents
580 in the fluid phase near 1 mole % and higher will be common for Plinian eruptions in
581 subduction zone settings. In such a situation, HCl adsorption on ash will not be able to
582 significantly reduce the amount of HCl reaching the stratosphere. Although there is
583 still much work to be done to understand these processes, previous studies (Textor et
584 al. 2003) have suggested limited efficiency of HCl scavenging by liquid water and by
585 ice in the eruption column, with more than 25 % of the total HCl reaching the
586 stratosphere. Our results therefore support the hypothesis that significant and perhaps
587 even catastrophic ozone depletion due to the HCl yield of giant eruptions is possible
588 (Kutterolf et al. 2013, Black et al. 2014).
589
590 **5. Conclusions**
591 The interaction of volcanic gases with ash particles could potentially limit the
592 environmental impact of explosive eruptions. We provide new experimental data on
593 the kinetics and thermodynamics of HCl adsorption on volcanic ash. Unlike for SO_2,
594 HCl adsorption increases with temperature, so that large temperature-dependent
595 fractionations between HCl and SO_2 occur during the adsorption process. Extracting
596 volcanic gas compositions from analyses of ash leachates therefore requires
597 correcting for this effect. Although HCl adsorption increases with temperature, the

598 slow rate of the process implies that most of the adsorption occurs in the cold, dilute
599 parts of a volcanic plume. For low initial HCl concentrations in the volcanic gas (0.1
600 mole % and below), the depletion of HCl by adsorption can be significant. However,
601 for HCl concentrations of 1 mole % and above, adsorption on ashes is unlikely to
602 reduce the stratospheric HCl yield of Plinian eruptions. Therefore, it appears quite
603 plausible that the HCl yield of large explosive eruptions may cause significant ozone
604 depletion in the stratosphere.
605

606 **Acknowledgements**

607 We would like to thank Gerti Gollner and Julia Huber for technical assistance in the
608 adsorption experiments and Lena Geiling for the determination of specific surfaces.
609 Constructive reviews by Tamsin Mather, Steffen Kutterolf and an anonymous referee
610 helped to improve the manuscript.
611

612 **References**

613 Armienta, M.A., Martin-Del-Pozzo, A. L., Espinasa, R., Cruz, O., Ceniceros, N.,
614 Aguayo, A., Butron, M.A., 1998. Geochemistry of ash leachates during the 1994-
615 1996 activity of Popocatépetl volcano. Appl. Geochem. 13, 841-850.
616 Armienta, M.A., de la Cruz-Reyna, S., Soler, A., Cruz, O., Ceniceros, N., Aguayo, A.,
617 2010. Chemistry of ash-leachates to monitor volcanic activity: An application to
618 Popocatépetl volcano, central Mexico. Appl. Geochem. 25, 1198–1205.
619 Ayris, P.M., Delmelle, P., Cimarelli, C., Maters, E.C., Suzuki, Y.J., Dingwell, D.B.,
620 2014. HCl uptake by volcanic ash in the high temperature eruption plume:
621 Mechanistic insights. Geochim. Cosmochim. Acta 144, 188-201.

622 Bagnato, E., Aiuppa, A., Andronico, D., Cristaldi, A., Liotta, M., Brusca, L.,
623 Miraglia, L., 2011. Leachate analyses of volcanic ashes from Stromboli volcano:
624 A proxy for the volcanic gas plume composition? J. Geophys. Res. 116, D17204,
625 DOI: 10.1029/2010JD015512.
626 Bagnato, E., Aiuppa, A., Bertagnini, A., Bonadonna, C., Cioni, R., Pistolesi, M.,
627 Pedone, M., Hoskuldson, A., 2013. Scavenging of sulphur, halogens and trace
628 metals by volcanic ash: The 2010 Eyjafjallajökull eruption. Geochim.
629 Cosmochim. Acta 103, 138-160.
630 Batzill, M., (2006) Surface science studies of gas sensing materials: SnO_2. Sensors 6,
631 1345-1366.
632 Black, B.A., Lamarque, J.F., Shields, C.A., Elkins-Tanton, L.T., Kiehl, J.T., 2014.
633 Acid rain and ozone depletion from pulsed Siberian Traps magmatism. Geology
634 42, 67-70.
635 Brasseur, G., Granier, C., 1992. Mount Pinatubo aerosols, chlorofluorocarbons, and
636 ozone depletion. Science 257, 1239-1242.
637 Brunauer, S., Deming, L.S., Deming, W.E., Teller, E., 1940. On a theory of the van
638 der Waals adsorption of gases. J. Am. Chem. Soc. 62, 1723-1732.
639 de Hoog, J.C.M., Koetsier, G.W., Bronto, S., Sriwana, T., van Bergen, M.J. 2001.
640 Sulfur and chlorine degassing from primitive arc magmas: temporal changes
641 during the 1982-1983 eruptions of Galunggung (West Java, Indonesia). J.
642 Volcanol. Geothermal Res. 108, 55-83.
643 Delmelle, P., Villiéras, F., Pelletier, M., 2005. Surface area, porosity and water
644 adsorption properties of fine volcanic ash particles. Bull. Volcanol. 67, 160-169.

645 Delmelle, P., Lambert, M., Dufrêne, Y., Gerin, P., Óskarsson, N., 2007. Gas/aerosol–
646 ash interaction in volcanic plumes: New insights from surface analyses of fine
647 ash particles Earth Planet. Sci. Lett. 259, 159–170.
648 Duran-Munoz, F., Romero-Ibarra, I., Pfeiffer, H. (2013) Analysis of the CO_2
649 chemisorption reaction mechanism in lithium oxosilicate (Li_8SiO_6): a new option
650 for high-temperature CO_2 capture. J. Materials Chem. A 1, 3919-3925.
651 Edmonds, E., Oppenheimer, C., Pyle, D.M., Herd, R.A., 2003. Rainwater and ash
652 leachate analysis as proxies for plume chemistry at Soufrière Hills volcano,
653 Montserrat. In: Oppenheimer, C., Pyle, D.M., Barclay, J. (eds) Volcanic
654 Degassing. Geological Society, London, Special Publications 213, 203-218.
655 Fischer, T. P., 2008. Fluxes of volatiles (H_2O, CO_2, N_2, Cl, F) from arc volcanoes.
656 Geochem. J. 42, 21-38.
657 Gislason, S. R., Hassenkam, T., Nedel, S., Bovet, N., Eiriksdottir, E. S., Alfredsson,
658 H. A., Hem, C. P., Balogh, Z. I., Dideriksen, K., Oskarsson, N., Sigfusson, B.,
659 Larsen, G., Stipp, S. L. S., 2011. Characterization of Eyjafjallajökull volcanic
660 ash particles and a protocol for rapid risk assessment. Proc Nat. Acad. Sci. USA
661 108, 7307-7312.
662 Halmer, M.M., Schmincke, H.U., Graf, H.F., 2002. The annual volcanic gas input into
663 the atmosphere, in particular into the stratosphere: a global data set for the past
664 100 years. J. Volcanol. Geothermal Res. 115: 511-528
665 Hofmann, D.J., Oltmans, S.J., Komhyr, W.D., Harris, J.M., Lathrop, J.A., Langford,
666 A.O., Deshler, T., Johnson, B.J., Torres, A., Matthews, W.A., 1994. Ozone loss
667 in the lower stratosphere over the United States in 1992 – 1993: Evidence for
668 heterogeneous chemistry on the Pinatubo aerosol. Geophys. Res. Lett. 21, 65-68.

669 Kutterolf, S., Hansteen, T.H., Appel, K., Freundt, A., Krüger, K., Pérez, W.,
670 Wehrmann, H. 2013. Combined bromine and chlorine release from large
671 explosive volcanic eruptions: A threat to stratospheric ozone? Geology 41, 707-
672 710.
673 Mankin, W.G., Coffey, M.T., 1984. Increased stratospheric hydrogen chloride in the
674 El Chicon cloud. Science 226, 170-172.
675 Mankin, W.G., Coffey, M.T., Goldman, A., 1992. Airborne observations of SO_2, HCl,
676 and O_3 in the stratospheric plume of the Pinatubo volcano in July 1991. Geophys.
677 Res. Lett. 19, 179-182.
678 Mather, T.A., McCabe, J.R., Rai, V.K., Thiemens, M.H., Pyle, D.M., Heaton, T.H.E.,
679 Sloane, H.J., Fern, G.R., 2006. Oxygen and sulfur isotopic composition of
680 volcanic sulfate aerosol at the point of emission. J. Geophys. Res. 111, Article
681 Number: D18205, DOI: 10.1029/2005JD006584
682 McCormick, M.P., Thomason, L.W., Trepte, C.R., 1995. Atmospheric effects of the
683 Mt Pinatubo eruption. Nature 373: 399-404.
684 Métrich, N., Wallace, P.J., 2008. Volatile abundances in basaltic magmas and their
685 degassing paths tracked by melt inclusions. Rev. Mineral. Geochem. 69, 363-402.
686 Millard, G. A., Mather, T. A., Pyle, D. M., Rose, W. I., Thornton, B., 2006. Halogen
687 emissions from a small volcanic eruption: Modeling the peak concentrations,
688 dispersion, and volcanically induced ozone loss in the stratosphere. Geophys.
689 Res. Lett., 33, Article number L19815, doi:10.1029/2006GL026959.
690 Oskarsson, N., 1980. The interaction between volcanic gases and tephra: fluorine
691 adhering to tephra of the 1970 Hekla eruption. J. Volcanol. Geoth. Res. 8, 251–
692 266.

693 Petersen, G.N., Bjornsson, H., Arason, P., 2012. The impact of the atmosphere on the
694 Eyjafjallajökull 2010 eruption plume. J. Geophys. Res. Atmospheres 117, DOI:
695 10.1029/2011JD016762.
696 Pyle, D.M., Mather, T.A., 2009. Halogens in igneous processes and their fluxes to the
697 atmosphere and oceans from volcanic activity: A review. Chem. Geology 263,
698 110-121.
699 Razouk, R.I., Salem, A.S., 1948. The adsorption of water vapor on glass surfaces. J.
700 Phys. Chem. 52, 1208–1227.
701 Robock, A., 2000. Volcanic eruptions and climate. Rev. Geophys. 38, 191-219.
702 Rose, W.I., 1977. Scavenging of volcanic aerosols by ash: Atmospheric and
703 volcanologic implications. Geology 5, 621-624
704 Rose, W.I., Millard, G.A., Mather, T.A., Hunton, D.E. Anderson, B., Oppenheimer,
705 C., Thornton, B.F., Gerlach, T.M., Viggiano, A.A., Kondo, Y., Miller, T.M.,
706 Ballenthin, J.O., 2006. Atmospheric chemistry of a 33–34 hour old volcanic
707 cloud from Hekla Volcano (Iceland): Insights from direct sampling and the
708 application of chemical box modeling. J. Geophys. Res. 111, article number
709 D20206, doi:10.1029/2005JD006872.
710 Schmauss, D., Keppler, H., 2014. Adsorption of sulfur dioxide on volcanic ashes.
711 Am. Mineral. 99, 1085–1094.
712 Solomon, S., Sanders, R.W., Garcia, R.R., Keys, J.G., 1993. Increased chlorine
713 dioxide over Antarctica caused by volcanic aerosols from Mount Pinatubo.
714 Nature 363: 245-248.
715 Solomon, S., Portmann, R.W., Garcia, R.R., Randel, W., Wu, F., Nagatani, R.,
716 Gleason, J., Thomason, L., Poole, L.R., McCormick, M.P., 1998. Ozone

717 depletion at mid-latitudes: Coupling of volcanic aerosols and temperature
718 variability to anthropogenic chlorine. Geophys. Res. Lett. 25, 1871-1874.
719 Symonds, R.B., Rose, W.I., Reed, M.H., 1988. Contributions of Cl- and F-bearing
720 gases to the atmosphere by volcanoes. Nature 334, 415-418.
721 Symonds, R.B., Rose, W.I., Bluth, G.J.S., Gerlach, T.M., 1994. Volcanic-gas studies:
722 Methods, results, and applications. Rev. Mineral. 30, 1-66.
723 Tabazadeh, A., Turco, R.P., 1993. Stratospheric chlorine injection by volcanic
724 eruptions: HCl scavenging and implications for ozone. Science, 260, 1082–1086.
725 Textor, C., Graf, H.F., Herzog, M., Oberhuber, J.M., 2003. Injection of gases into the
726 stratosphere by explosive volcanic eruptions. J. Geophys. Res. 108, Article
727 number 4606, doi:10.1029/2002JD002987.
728 Textor, C., Graf, H.F., Herzog, M., Oberhuber, J.M., Rose, W.I., Ernst, G.G.J., 2006.
729 Volcanic particle aggregation in explosive eruption columns. Part II: Numerical
730 experiments. J. Volcanol. Geothermal Res. 150, 378-394.
731 Thamban, M., Chaturvedi, A., Rajakumar, A., Naik, S.S., D´Souza, W., Sing, A.,
732 Rajan, S., Ravindra, R., 2006. Aerosol perturbations related to volcanic eruptions
733 during the past few centuries as recorded in an ice core from the Central
734 Dronning Maud land, Antartica. Current Science 91, 1200-1207.
735 Wagnon, P., Delmas, R. J., Legrand, M., 1999. Loss of volatile acid species from
736 upper firn layers at Vostok, Antarctica. J. Geophys. Res. 104, 3423–3431.
737 Wallace, L., Livingston, W., 1992. The effect of the Pinatubo cloud on hydrogen-
738 chloride and hydrogen-fluoride. Geophys. Res. Lett. 19, 1209-1209.
739 Williams, S.N., Stoiber, R.E., Garcia, N., Londono, A., Gemmel, B.C., Lowe, D. R.,
740 Connor, C.B., 1986. Eruption of the Nevado des Ruiz volcano, Colombia on 13
741 November 1985: Gas flux and fluid geochemistry. Science 233, 964-967.

742 Woods, A.W., Bursik, M. I., 1991. Particle fallout, thermal disequilibrium and
743 volcanic plumes. Bull. Volcanol. 53, 559-570.
744 Woods, D.C., Chuan, R.L., Rose, W.I. , 1985. Halite particles injected into the
745 stratosphere by the 1982 El Chicón eruption. Science 230, 170-172.
746 Zdanowicz, C. M., Zielinski, G. A., Germani, M. S., 1999. Mount Mazama eruption:
747 Calendrical age verified and atmospheric impact assessed. Geology 27, 621– 624.
748

749 **Table 1**

750 Chemical composition (wt. %) and specific surface A (m^2/g) of synthetic glass
751 samples and of a natural obsidian from Vulcano (Aeolian Islands, Italy) used for
752 adsorption experiments

	Rhyolite	Dacite Batch 1	Dacite Batch 2	Dacite Batch 3	Andesite	Vulcano Obsidian
SiO_2	76.45 (83)	67.08 (30)	67.02 (49)	66.68 (71)	56.77 (18)	73.47 (35)
Al_2O_3	12.37 (53)	16.49 (21)	16.81 (23)	16.96 (32)	21.63 (13)	13.49 (22)
Fe_2O_3 (t)						1.86 (13)
MgO	3.14 (24)	4.96 (15)	4.97 (23)	5.14 (37)	7.31 (16)	0.11 (04)
CaO	0.80 (07)	2.80 (10)	2.93 (11)	2.86 (16)	7.46 (10)	0.83 (10)
Na_2O	2.77 (08)	4.31 (09)	4.20 (05)	4.46 (09)	3.88 (09)	4.42 (08)
K_2O	3.33 (05)	3.15 (06)	3.00 (06)	2.92 (07)	1.77 (06)	5.10 (05)
Total	98.86	98.79	98.93	99.02	98.82	99.28
A	3.82	4.90	1.50	2.74	3.01	2.97

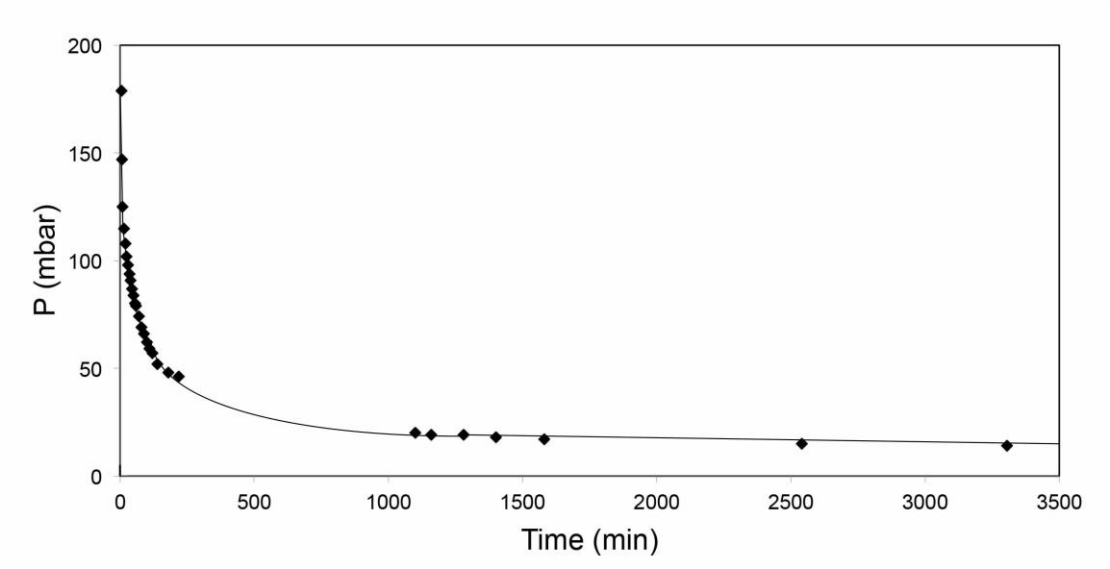
753 Numbers in parentheses are one standard deviation in the last digits. Fe_2O_3 (t) is the
754 total iron content given as Fe_2O_3. For dacite, three batches of sample were prepared.
755 Batch 1 was used for experiments at room temperature, batch 2 at 150 ˚C, and batch 3
756 at -76 ˚C. Note that the synthetic compositions do not necessarily correspond to
757 global averages of the respective rock type.

Table 2

Rate constants λ for the adsorption of HCl on glass surfaces

Andesite		Dacite						Rhyolite	
T = 22 ˚C		T = - 76 ˚C		T = 22 ˚C		T = 150 ˚C		T = 22 ˚C	
p (mbar)	λ (10^{-6} s^{-1})	p (mbar)	λ (10^{-6} s^{-1})	p (mbar)	λ (10^{-6} s^{-1})	p (mbar)	λ (10^{-6} s^{-1})	p (mbar)	λ (10^{-6} s^{-1})
68	124 (48)	58	58.5 (3.6)	42	180 (24)	104	44.4 (1.3)	80	45.4 (5.5)
105	52.1 (11.2)	86	103 (9)	147	32.1 (1.4)	95	15.9 (0.5)	125	57.0 (9.7)
185	44.3 (9.3)	123	96.7 (6.4)	197	12.0 (0.3)	315	14.8 (1.1)	191	149 (3)
374	28.2 (8.1)	206	99.4 (6.3)	306	5.98 (1.41)	424	6.92 (0.28)	243	37.7 (13.7)
581	42.8 (11.4)	299	103 (7)	528	6.32 (0.27)	538	25.4 (0.3)	371	43.0 (17.0)
721	117 (23)	529	92.6 (10.7)	692	7.58 (0.72)	798	21.8 (25.8)	506	46.3 (14.1)
852	58.6 (10.2)	723	66.2 (30.0)	794	2.75 (7.06)	956	18.1 (19.0)	713	34.0 (12.6)
982	36.4 (15.7)	935	76.1 (23.3)	965	2.13 (0.43)			967	37.3 (14.5)

p is the initial pressure of HCl vapor to which the sample was exposed in each step. The pressures are listed in the sequence of the steps of the adsorption experiment. Numbers in brackets are estimated uncertainties.



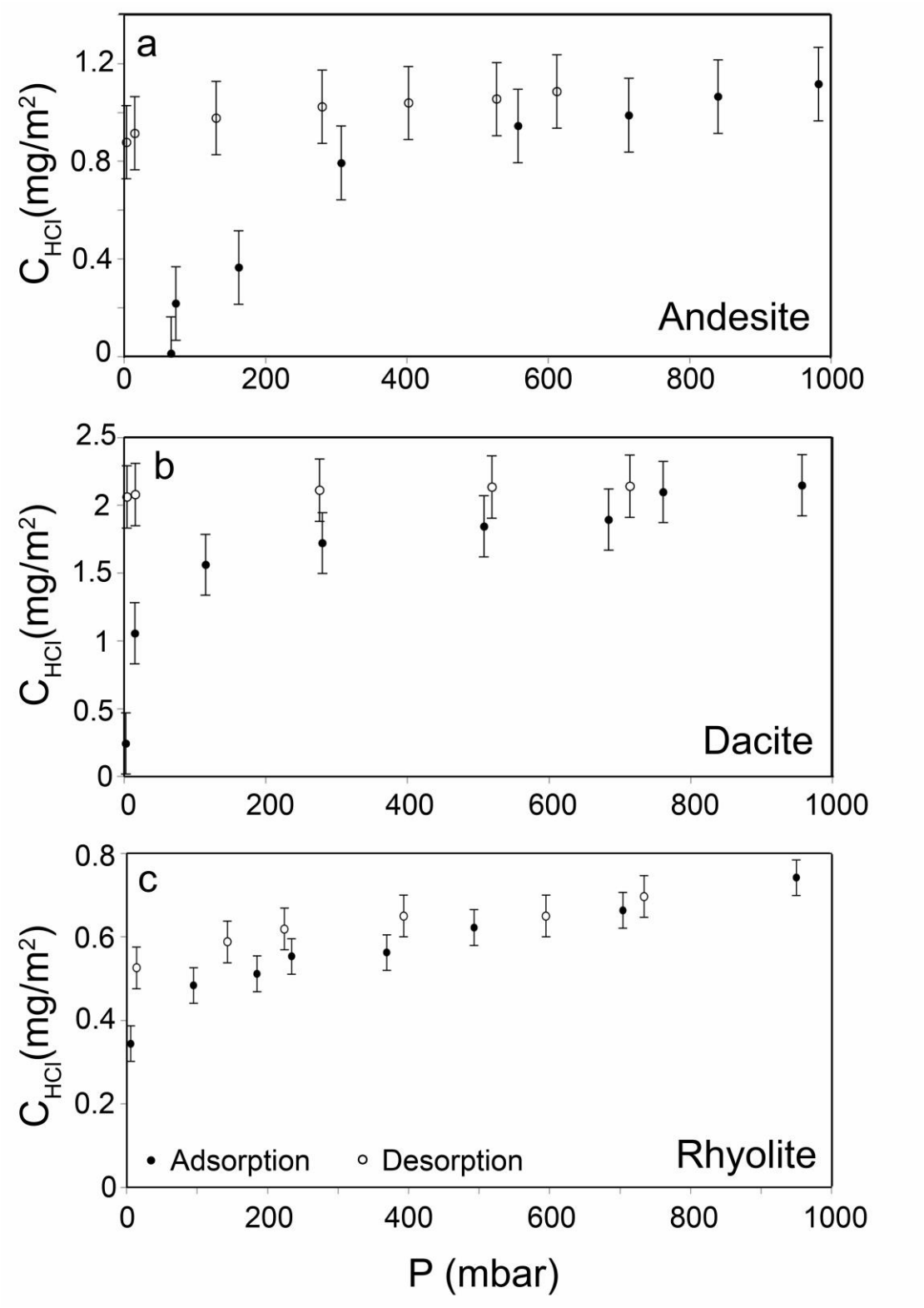
762

763

764 **Fig. 1.** Kinetics of HCl adsorption on dacitic glass at room temperature and for an

765 initial pressure p_0 = 179 mbar. Pressure in the system decreases exponentially, until

766 equilibrium is reached.



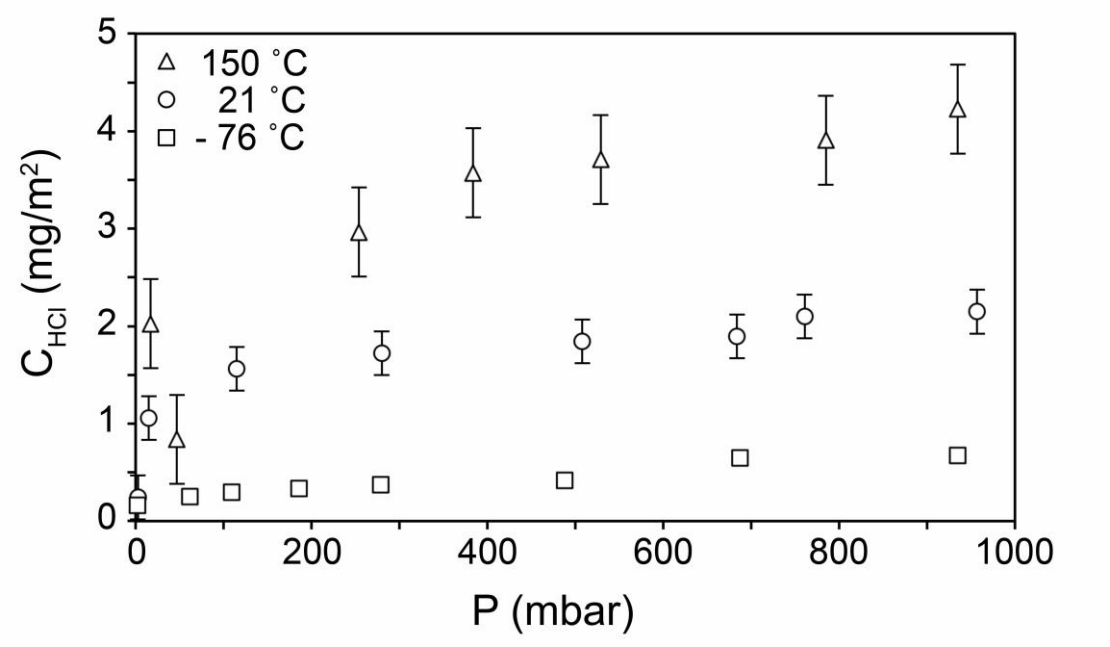
767

768

769 **Fig. 2.** HCl adsorption and desorption isotherms for (a) andesitic, (b) dacitic, and (c)

770 rhyolitic compositions at room temperature. Error bars are one standard deviation.

771

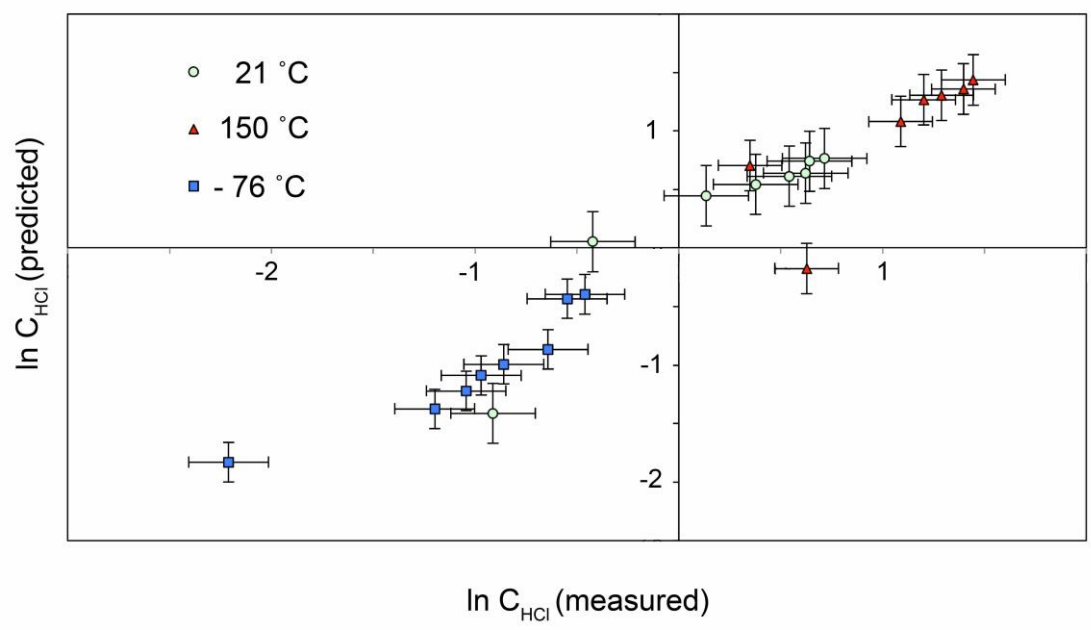


772

773 **Fig. 3.** Effect of temperature on the adsorption of HCl on dacite glass. Error bars are

774 one standard deviation.

775

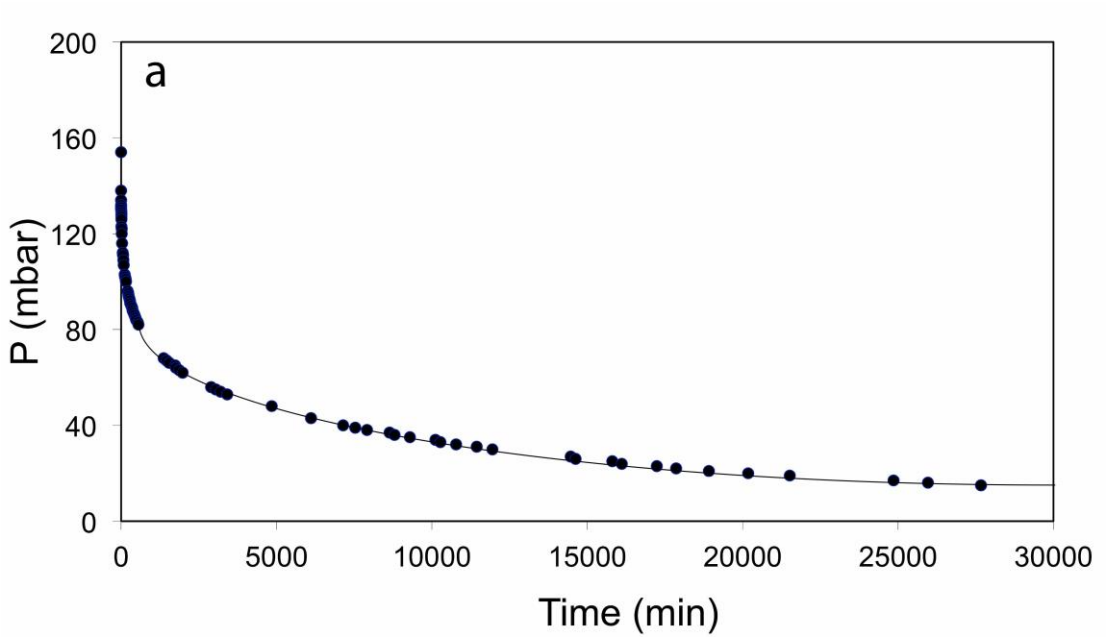


776

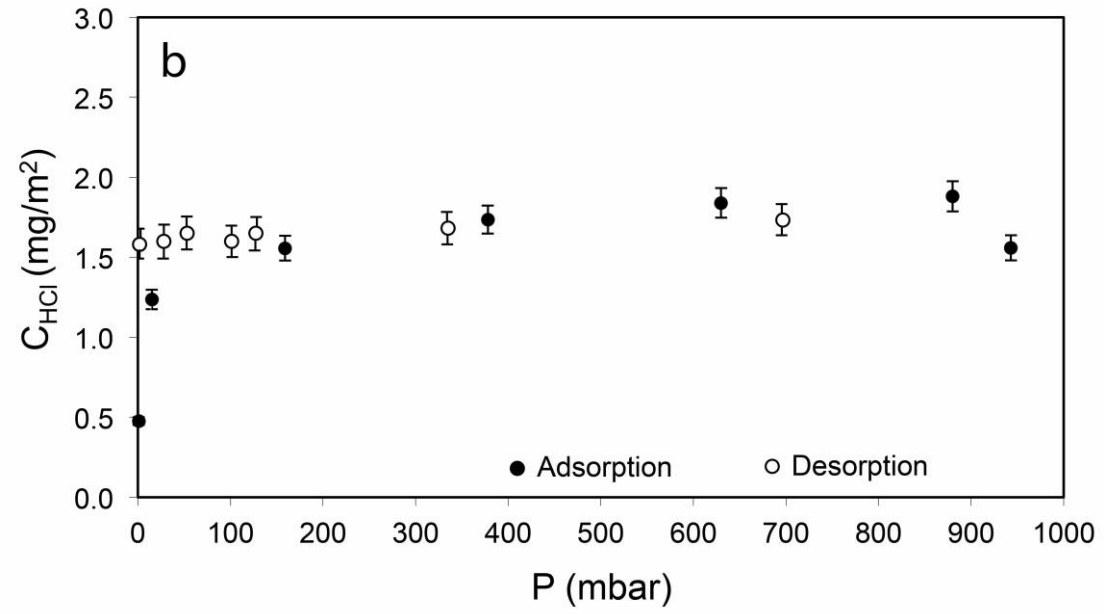
777 **Fig. 4.** Multiple regression model for the adsorption of HCl on dacite glass. Surface

778 concentrations c are in mg/m^2.

779



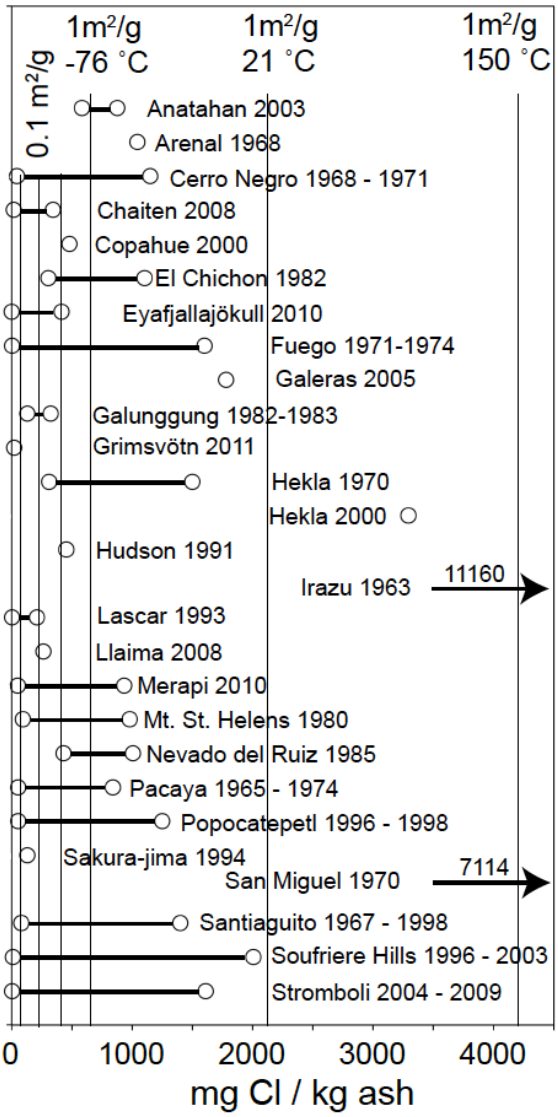
780



781

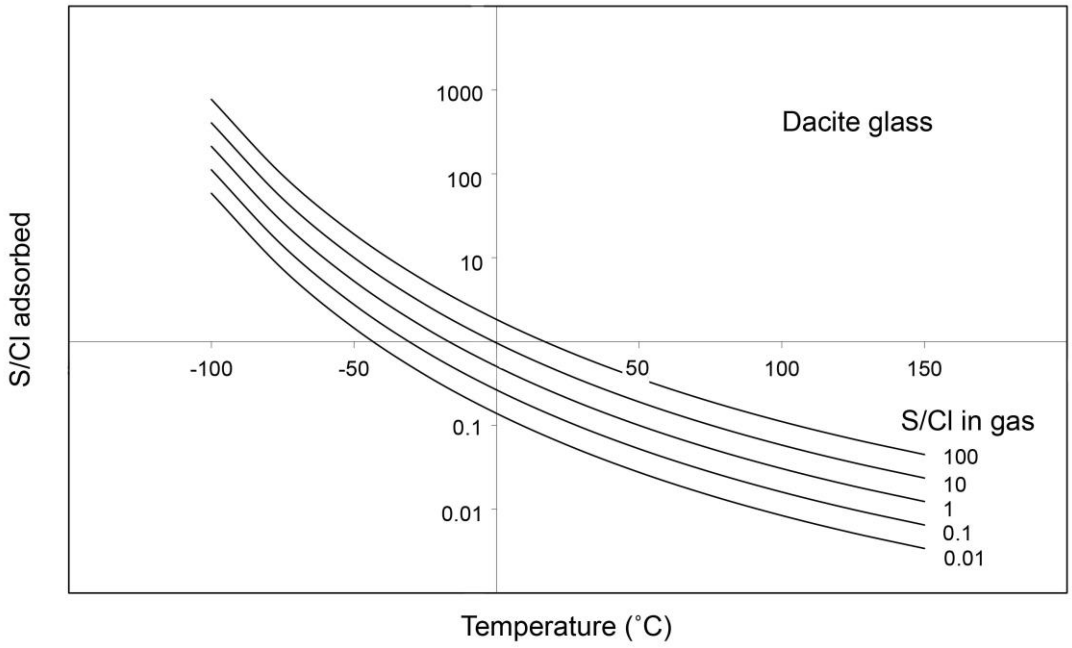
782 **Fig. 5.** HCl adsorption on a natural obsidian from the 1739 A.D. eruption of Vulcano
783 (Aeolian Islands, Italy). a) Kinetics of adsorption at room temperature for an initial
784 pressure of p_0 = 138 mbar. The decrease in pressure can be described by a rate
785 constant of $\lambda = 1.28 \cdot 10^{-5}$ s^{-1}; b) Adsorption and desorption isotherms at room
786 temperature. Error bars are one standard deviation. The point at the highest pressure
787 may have been affected by some unknown experimental problem.

788



789

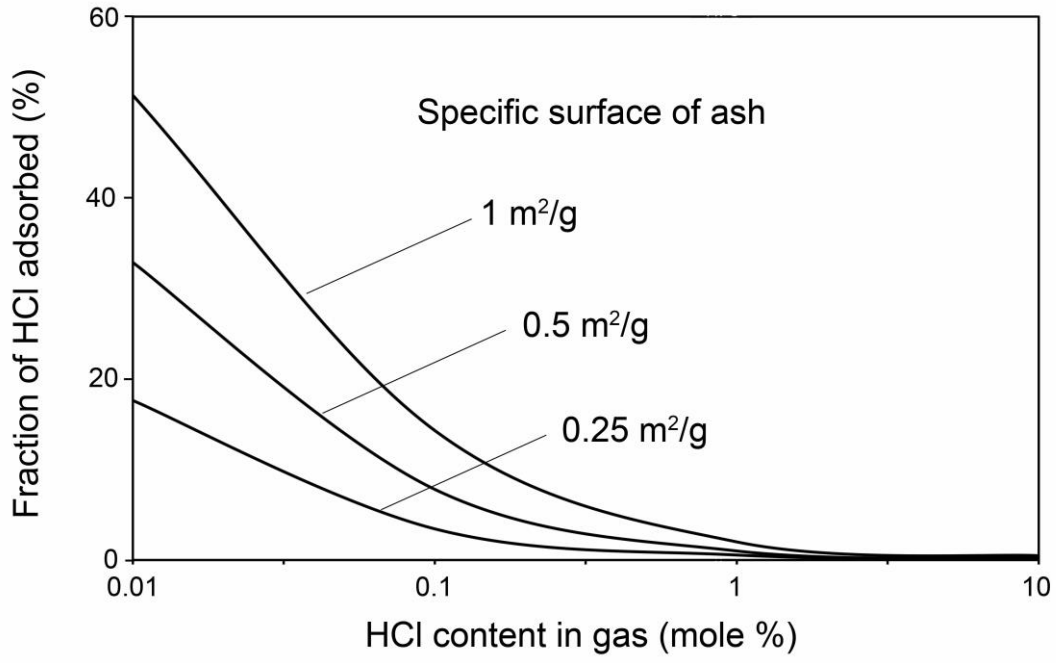
790 **Fig. 6.** Concentrations of chlorine adsorbed on volcanic ashes from recent eruptions
791 (see supplementary Table S2 for data and sources). The data are compared with the
792 maximum surface concentrations according to the experimental data for HCl
793 adsorption on dacite glass (vertical lines), assuming two different specific surface
794 areas (1 m^2/g for fine ash, 0.1 m^2/g for coarser ash) and adsorption at three different
795 temperatures (150 ˚C, 21 ˚C, -76 ˚C). Note that some samples may contain a
796 contribution of Cl-bearing alteration products from other sources, e.g., evaporites,
797 marine aerosols or pre-eruptive interaction with saline groundwaters, altered dome
798 rocks or recycled volcanic ejecta.



799

800 **Fig. 7.** Calculated fractionation of SO_2 and HCl between volcanic gas and the surface
801 of dacitic ash as a function of temperature.

802



803

804 **Fig. 8.** Fraction of HCl adsorbed on volcanic ash in the umbrella part of a
805 stratospheric plume as a function of initial HCl concentration in the volcanic gas.
806 Assumptions: Plume altitude 20 km, temperature 220 K, dilution factor 200.